NEW INSIGHTS INTO PREDICTING THE FATIGUE RANKING OF STEEL WELDS

M. N. James[1, 2], S.-P. Ting[1], M. Bosi[3], H. Lombard[2] and D. G. Hattingh[2]

[1] School of Engineering, University of Plymouth, Drake Circus, Plymouth (UK)
[2] Department of Mechanical Engineering, Nelson Mandela Metropolitan University, Port Elizabeth (South Africa)
[3] Department of Engineering, University of Ferrara, Ferrara, (Italy)
E-mail: mjames@plymouth.ac.uk; mbosi@ing.unife.it

ABSTRACT

This work has investigated the potential for information contained in the residual transverse strain and microhardness profiles to predict the fatigue performance ranking for a series of 12 MIG welds made in RQT701 steel under different conditions. The experimental matrix included two plate thicknesses, two heat inputs and three types of filler metal. Predictive modelling considered the use of a number of parameters that might characterise the effect of residual strain and microhardness profiles on fatigue performance, including maximum range experienced at the toe, gradients associated with the weld toe, and changes in these parameters across the weld toe. It proved possible to predict the fatigue ranking at a life of 10^5 cycles for 10/12 of the weld conditions tested, based on weld toe hot spot strain and a combination of residual strain range at 1 mm depth and the hardness range at mid-depth. Relationships were observed between the measured parameters and fatigue performance at lives of $2x10^6$ cycles but additional discriminating parameters are required to predict fatigue ranking.

1. INTRODUCTION

The sub-critical cracking performance of structures fabricated from higher strength steel depends strongly on the role played by welded joints and connections in influencing fatigue crack initiation and growth. Typical applications of higher strength steels include the tubular sections (with wall thickness from 8 mm up to >60 mm) used in fabrication of bridge and offshore structures which are exposed to low cycle fatigue situations where significant engineering benefit derives from their higher tensile strength. The design life of welded steel structures in Europe is based on generic and therefore conservative codes similar to BS 7608: 1993 [1]. This conservative approach is justified by observations that the fatigue performance of welded joints can be both batch and fabricator dependent, even for simple geometries made under nominally similar process conditions.

It is also known that fatigue life of welded joints generally decreases as section thickness increases and that these effects are influenced by tensile strength level of the steel. The effects of steel thickness and strength level on fatigue performance of welded joints reflect heat input, heat flow, and the resulting microstructural, hardness and residual strain gradients across the weld zone. A considerable body of work has been published dealing with the

measurement of residual stresses and their relaxation under cyclic loading, e.g. [2-7], or with fatigue crack initiation and growth as a function of weld notch effects and microstructure, e.g. [8-10]. Despite these results, it remains difficult to interpret the fatigue performance of specific joint geometries in higher strength steels, or to make precise predictions of residual strains and stresses. Indeed, it has not been possible to predict the relative fatigue ranking of joints made in one steel alloy using various levels of heat input, filler metal strength and plate thickness.

If the underlying causes of variable fatigue performance between nominally similar joints were better understood, predictive capability could be improved, particularly for the important case of higher strength steel structures. However, welding will always possess a high parametric potential for local property variability, and prediction of fatigue life is likely to remain statistically imprecise. More usefully, it may be possible to assess the effect of changes in joint design or weld process parameters on fatigue performance at specific lives through a ranking process.

This paper presents the outline of a fatigue performance ranking process for MIG welds in higher strength steel plate based on easily measurable and physically meaningful parameters that characterise the effects of alloy metallurgy and the weld thermal cycle. As will be seen, it is then possible to predict, with some success, the relative fatigue ranking of joints made in one steel alloy using various levels of heat input, filler metal strength and plate thickness.

2. FATIGUE PREDICTION PHILOSOPHY

This work described in this paper has explored the potential for predicting the fatigue ranking order of a number of different fusion welds in higher strength steel at fatigue lives of around 10^5 cycles and $2x10^6$ cycles. A roller quenched and tempered steel grade (RQT701) has been used in plates either 8 mm or 12 mm thick. This steel has a nominal yield strength >690 MPa and a tensile strength in the range 790-930 MPa. Welds were made between plates 1 m long and 150 mm wide using two values of heat input (with different numbers of weld runs) and three types of filler metal. This provided a matrix of 12 welded plates made with different heat input, heat flow and filler metal and hence giving quite variable weld zone extent, microstructure, hardness, residual strain and tensile properties. The steel was supplied and the welds made through the Swindon Technology Centre of the Corus Group.

The aim of the study was to predict the fatigue ranking of the welds, assessed using stress-life or strain-life (S-N) data representing either applied elastic stress across the weld, weld toe hot spot stress or weld toe hot spot strain. The philosophy underlying the predictive process is that fatigue performance in these welds is dominated by strength/hardness and residual strain gradients across the weld toe, which is almost invariably the site of crack initiation in un-ground fusion welds. The relative influence of these parameters and their gradients, which are induced through alloying, metallurgical and heat flow phenomena, will vary with cyclic life to failure (N_f), i.e. with the relative extent of the crack initiation and growth stages in the fatigue process. Hence this approach is physically meaningful and allows for discriminating between the relative influences of crack initiation and crack growth in the overall fatigue life.

Hardness and tensile strength are known to influence crack initiation and growth in opposite ways; higher values of hardness/strength are beneficial in terms of countering crack initiation, but usually lead to higher crack growth rates. Both of these effects can be related to the

dimension of the controlling microstructural parameter (grain size, bainite packet size etc) which generally decreases as strength or hardness increases.

Residual strain/stress influence both crack initiation and growth phases of life in a similar manner by decreasing the number of cycles necessary to achieve a crack of a given length. High positive magnitudes of residual strain decrease the crack initiation life under a given stress amplitude [11] due mainly to the increased mean stress in the fatigue cycling, although presumably a ratchetting effect can occur depending on alloy and stress conditions [12]. High positive magnitudes of residual strain also increase crack growth rate via mean stress effects, at least up to mean stress values equivalent to a stress ratio $R > 0.7$.

Although the principle of assessing fatigue performance from hardness/strength and residual strain gradients is straightforward, there are number of practical, experimental and interpretative difficulties. Included amongst these are accurate and precise quantification of the residual strain values through the thickness of the plate and identifying an appropriate gradient, or change in gradient, at the weld toe in hardness and strain profiles of complex shape. Finally, there are a large number of possible permutations of various parameters to consider in identifying statistically meaningful relationships.

The rest of this paper outlines the procedures followed and the rationale behind their use and demonstrates that the parameters of hardness and residual strain gradient can be used to correlate the hot spot strain fatigue behaviour of 10/12 welds at lives ~ 10^5 cycles and to identify trends in fatigue performance of 11/12 welds at lives ~ $2x10^6$ cycles.

3. ALLOY AND WELD PROCESS PARAMETERS

Mechanical property data for the RQT701 steel is given in Table 1. Welds were made using filler metal with a tensile strength that overmatched, matched or undermatched (respectively indicated in this paper by O, M and U) the parent plate tensile strength, and two different heat inputs of either 1 kJ/mm (low input - L) or 3 kJ/mm (high input - H). These heat input figures lie within the envelope stipulated by BS 7191: 1989 for offshore use (0.7 kJ/mm and 3.5 kJ/mm). Low heat input gives small welds with high hardness due to fast cooling rates and higher preheat may be required to achieve a satisfactory weld. High heat inputs give faster production rates but can give poor heat-affected zone (HAZ) mechanical properties due to grain growth. The heat input values were chosen to provide a range of weld microstructures and mechanical properties representative of service conditions.

Table 1: *Mechanical properties of the RQT701 steel.*

Plate Thickness mm	Yield Stress MPa	Tensile Strength MPa	Elongation on 50 mm GL %	Charpy V-Notch Average J @ ºC	Charpy V-Notch Individual J @ ºC
$6 \le t \le 40$	> 690	790-930	> 18	> 27 @ -40	> 20 @ -40
8	794	831	16	33	29 35 34
12	801	846	18	46	39 40 59

These parameters gave a matrix of six different weld process conditions for each plate thickness (referred to, for example, as U8L in this paper) and allow a systematic examination

of the variation across the weld zone in residual strain and hardness profiles as a function of process conditions. Table 2 gives the specified mechanical properties of the three filler metal grades used in this study. Figure 1 shows details of the multipass MIG welding used to make the butt joints in the 8 mm and 12 mm plate. The shielding gas comprised a mixture of 80% argon and 20% carbon dioxide. Run-on and run-off tabs were used, with no preheat and maximum interpass temperatures of 250ºC and heat input values of either 1 kJ/mm or 3 kJ/mm.

Table 2: *Specified properties for the three filler metal alloys.*

Filler Metal Type	Yield Stress MPa	Tensile Strength MPa	Elongation %	Charpy V-Notch J @ ºC
O Fluxofil 45 - Flux cored	980	1070	15	55 @ -20
M Fluxofil 42 - Flux cored	695	800	17	70 @ -40
U Carbofil 1 - Solid wire	500	605	21	60 @ -20

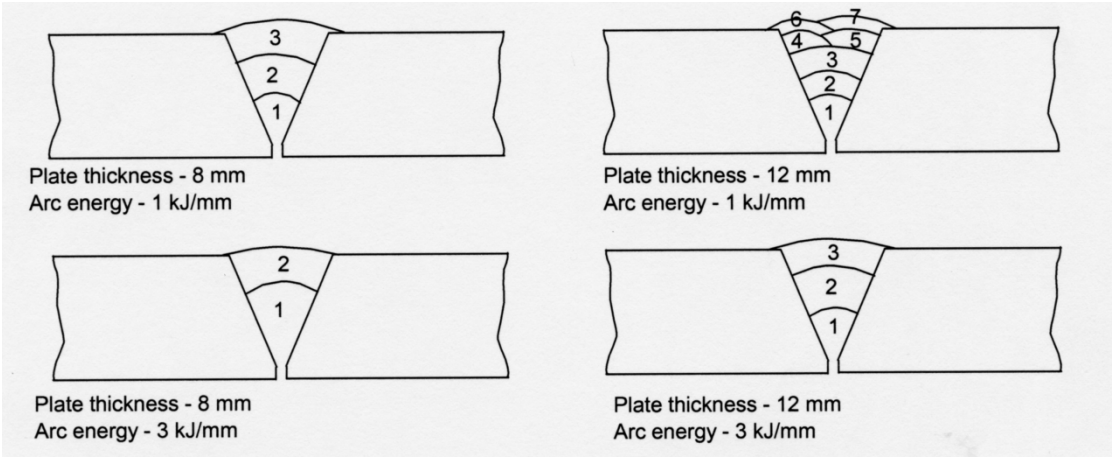

Figure 1*:* Details of the multipass weld runs used to make the butt joints in the 8 mm and 12 mm thick plates of RQT701 steel.

4. WELD ZONE MECHANICAL PROPERTIES

The weld zone mechanical properties of interest in this work were the hardness of the microstructure and the yield strength of the weld metal. These two properties are highly variable across the weld zone and generally correlate with each other, although the yield strength may be a more sensitive indicator of fatigue performance. Tensile properties were measured at one position in the centre of the weld metal using a standard tensile test on a 2.5 mm diameter waisted specimen. Thus the primary output from these tests was an indication of the extent to which choice of filler metal can determine if the weld is overmatched, matched or undermatched with respect to the yield strength of the parent plate. The 1 m by 0.3 m welded plates supplied by Corus were cut up to provide specimens for residual strain measurement, metallurgical analysis and fatigue testing. Figure 2 shows the cutting diagram

for the U8L (W3A5) weld and indicates the specimens used for residual strain scanning, and for metallurgical sectioning and tensile testing.

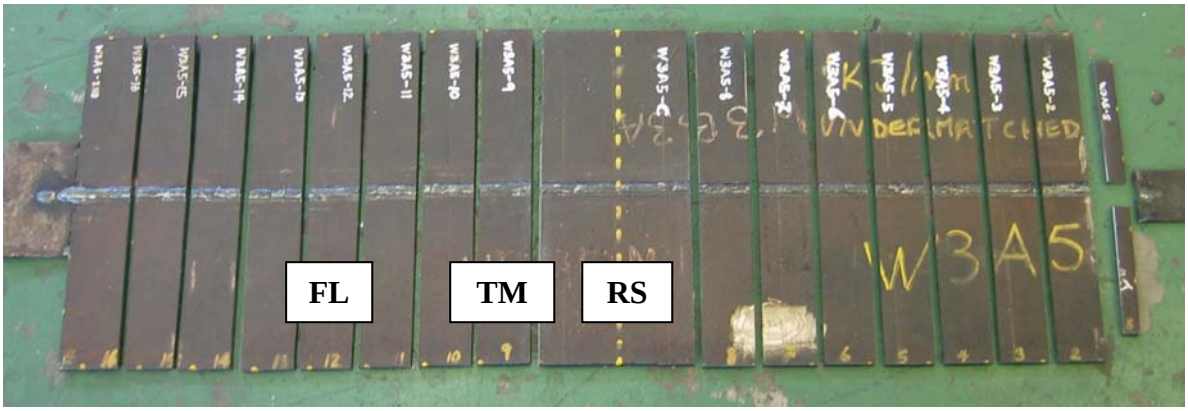

Figure 2: Cutting diagram for the welded plates, the residual strain specimen is marked with RS, the tensile strength/microstructure specimen is marked with TM and a typical fatigue specimen is marked as FL.

Table 3 gives the relevant tensile data for the various combinations of weld parameters used in this study. It is clear that the concept of undermatched, matched and overmatched filler metal does not translate in a straightforward way to the actual strength of the fusion zone in these multipass welds.

The effect of heat input and heat flow (plate thickness) on microstructure across the weld zone was characterised using microhardness mapping with a Vickers diamond indenter and a 500gf load. Mapping was performed along horizontal lines 1 mm below the plate surface and on the mid-section plane. These positions were chosen from consideration of discriminating whether the prime microstructural influence would be on either crack initiation from possible weld toe intrusions or undercut (perhaps ~ 1 mm below the surface), or on crack growth where mid-depth microstructure may dominate. An automated Buhler Omnimet system was used and the microhardness data were smoothed using a 3-point sliding average technique.

Typical data are shown in Figure 3 for the U12H and U8H welds overlaid on macrographs of the weld microstructures. Peaks in the hardness data correlate closely with weld interpass, fusion zone and heat affected zone (HAZ) boundaries and this is generally true for all the welds. These data are representative of all the undermatched welds where the mid-depth hardness exhibits greater values in fusion zone than at the 1 mm depth position. This reflects the slower cooling rate associated with the capping runs.

The trends in hardness data are more variable for the matched cases, reflecting the trends seen in the tensile data given in Table 3 and hardness values in the fusion zone vary between the two positions with filler metal and heat input. All the overmatched welds exhibit higher values of hardness across the fusion zone at the 1 mm plane. Representative data for the M8H weld (W3A9) and the O8L (W3A18) welds are given in Figure 4.

Table 3: *Measured weld metal tensile data for the various combinations of weld parameters.*

Weld Process Conditions							Plate ID	0.1% Proof Strength MPa	Tensile Strength MPa
Heat Input		Filler Metal Type			Plate Thickness				
1 kJ/mm	3 kJ/mm	U	M	O	8 mm	12 mm			
X		X			X		W3A5	477	692
	X	X			X		W3A4	368	585
X			X		X		W3A12	637	880
	X		X		X		W3A9	565	885
X				X	X		W3A18	663	944
	X			X	X		W3A14	598	838
X		X				X	W3A6	474	606
	X	X				X	W3A3	398	646
X			X			X	W3A11	687	854
	X		X			X	W3A8	575	805
X				X		X	W3A17	880	1028
	X			X		X	W3A13	602	940

In all cases, the weld toe corresponds with a turning point in the hardness profile and there are therefore several parameters that may be relevant to interpreting how change in hardness might affect fatigue crack growth, including the gradients and magnitudes of the two segments of the profile either side of the turning point and the change in gradient at the turning point. The parameter that gave the best results in the predictive modelling was the maximum range of hardness experienced at the weld toe. This is in physical agreement with the well known concept of a “metallurgical notch” caused by localised variation in hardness, which increases the likelihood of crack initiation and early crack growth. Results from the predictive modelling exercise are summarised in section 7 below.

5. RESIDUAL STRAIN MEASUREMENTS

The strain scanning specimen shown in Figure 2 measures 150 mm along the weld and has the full plate width of 300 mm. This should be large enough to retain residual strains representative of the full size plate. Residual strains were measured transverse to the weld run at a matrix of points on the central transverse plane through the weld, i.e. 75 mm along the weld run. Measurements were made at the same depth positions as the microhardness scans, i.e. 1 mm below the surface of the plate and mid-depth, using neutron diffraction strain scanning on the SALSA instrument at the ILL, Grenoble. The experimental details were largely the same as those reported in reference 13 for some earlier exploratory strain scanning work on these specimens.

The transverse stresses/strains are likely to be influential in crack initiation and appear to reflect the sequence of weld runs more than the longitudinal stresses. Full details of these results are available in [14]. These welds contain longitudinal residual stresses up to the level of parent plate yield strength and transverse residual stresses >50% of the parent plate yield

strength. These will vary considerably with weld conditions, plate thickness and measurement position and it would therefore be expected that the fatigue performance would reflect their influence.

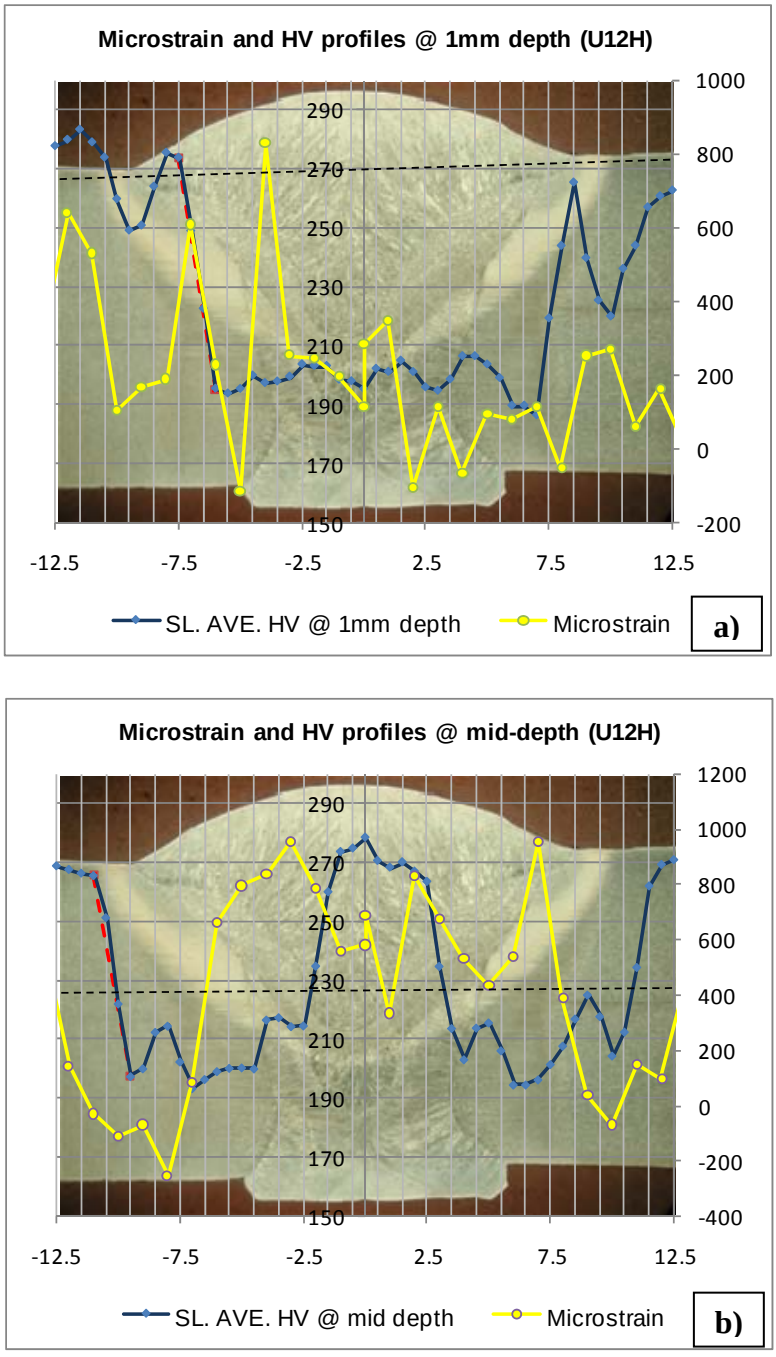

Figure 3: Microstrain and hardness profiles for the U12H (W3A3) weld: a) at a depth of 1 mm below the weld toe and; b) at mid-depth (6 mm below the weld toe).

In the present work, the beamtime allocation was sufficient to measure the transverse strains in all 12 specimens along two lines using a matrix of points with 1 mm intervals from the weld centreline to ±20 mm and then 2 mm intervals to -30 mm and +60 mm. In terms of

assessing whether strain gradients and magnitudes across the weld toes can be related to fatigue performance, the critical region lies between ±20 mm.

In trying to interpret residual strain data across weld zones with graded microstructures it is essential to identify how the strain-free lattice spacing d_0 varies across the weld zone. Thus after the residual strain measurements were completed a 2 mm thick section was cut from each specimen across the weld zone and a "toothcomb" specimen was prepared for separate d_0 measurement [15]. Reference 14 gives details of the d_0 measurements which were performed using synchrotron diffraction strain scanning on the ESRF instrument ID31 at Grenoble and contains a table showing the necessary corrections to residual strains in the fusion zone of the welds. Lattice spacing in these steels appears to depend more strongly on weld metal composition than on heat input and heat flow, and the strain correction data correlated well with the chemical composition data for the filler metals.

Typical residual strain data are also shown in Figure 3 (weld U12H W3A3) and Figure 4 (weld O8L W3A18) superimposed on the macrographs and microhardness profiles. The data have been smoothed using a 3-point sliding average technique. As was observed for the microhardness data, turning points in the residual strain profiles generally correspond with boundaries between weld passes, fusion zone and HAZ, or HAZ and parent plate. Data are highly variable between welds and at the two plate depths considered. Hence any derived relationship between residual strain, microhardness and fatigue life is likely to reflect genuine influences of importance to weld performance.

6. FATIGUE PERFORMANCE OF THE WELDS

The welds were tested in 4-point bend with a stress ratio $R = 0.2$. Fatigue specimens had a width of 40 mm and their length corresponded with the full width of the welded plate, as indicated in Figure 2. This size of specimen should retain a substantial level of residual strain transverse to the weld run and their fatigue performance should therefore reflect residual strain and microhardness influences across the weld toe. Fatigue performance and ranking of the welds was assessed using S-N data based on three techniques, nominal elastic stress range, hot spot stress at the weld toe and hot spot strain at the weld toe. A set of fatigue tests was performed to acquire nominal elastic stress S-N data for all the weld conditions and these data were subsequently processed to yield equivalent hot spot stress and hot spot strain data and details of this processing are given in reference 14.

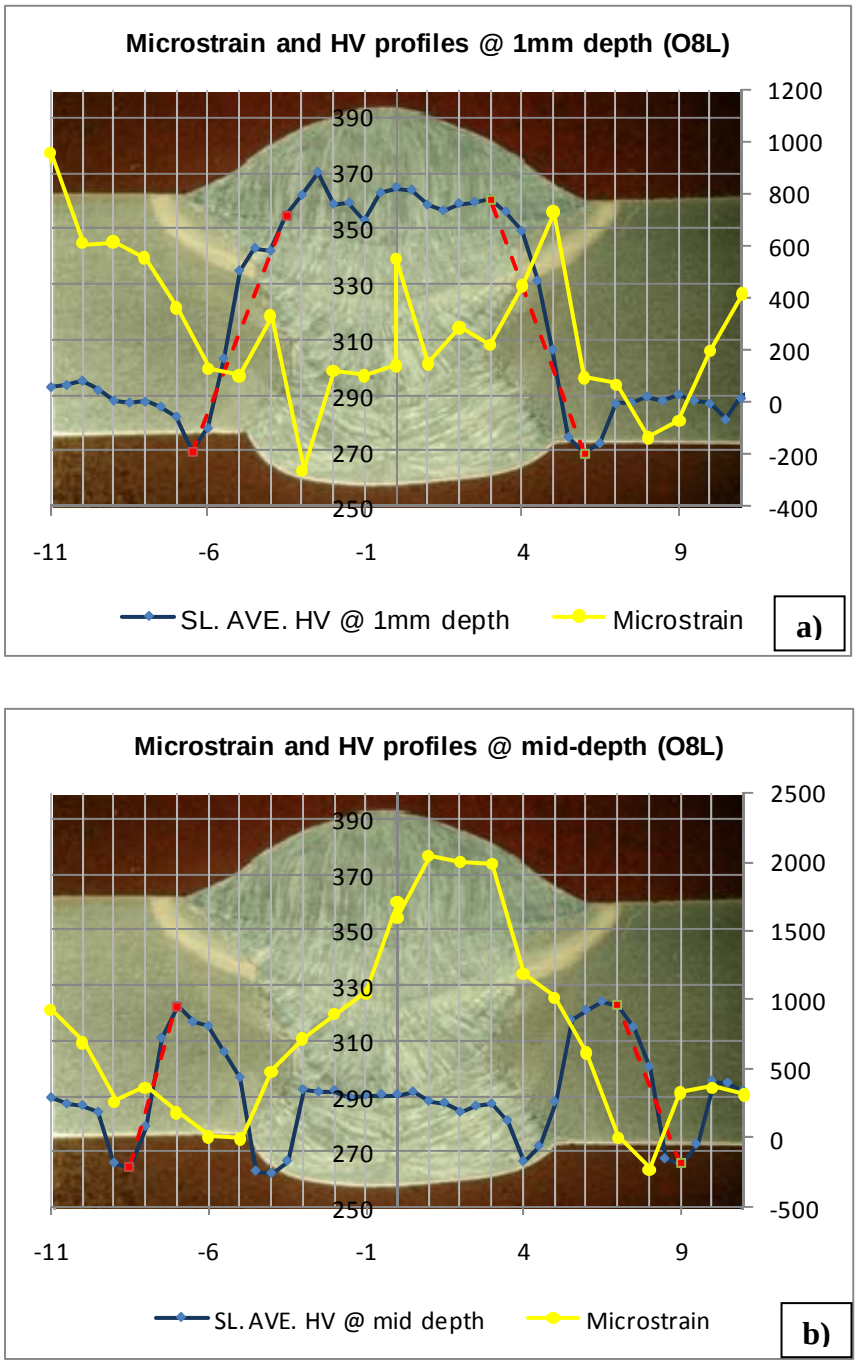

Figure 4: Microstrain and hardness profiles for the O8L (W3A18) weld: a) at a depth of 1 mm below the weld toe and; b) at mid-depth (4 mm below the weld toe).

In the modelling process, it became apparent that hot spot strain fatigue ranking of the various welds gave the best correlation with residual strain and microhardness profiles across the weld toe (which was the expected result), so attention will be focussed only on those results in this paper. Typical hot spot strain S-N data for the overmatched welds are presented in Figure 5 and reference 14 gives complete data for all 3 filler metals. In terms of fitting trend lines to

the data, insufficient material was available during this project to ascertain unequivocally whether bi-linear fitting or a polynomial expression would be most appropriate. Nonetheless, sufficient data is available to determine a fatigue ranking of the welds at specific lives of 10^5 cycles and $2x10^6$ cycles. These values are chosen as being representative of shorter and longer fatigue lives; $2x10^6$ cycles is widely used in fatigue design codes for this purpose. It is useful to distinguish between low cycle and high cycle fatigue ranking, as geometrically similar welds often show a crossover in fatigue ranking in going from shorter to longer lives. This particular aspect of weld behaviour probably reflects the increasing relevance of crack initiation and early growth to overall performance in the long life regime and is not considered in current codes, where design curves are generically applicable to a specific joint geometry irrespective of life.

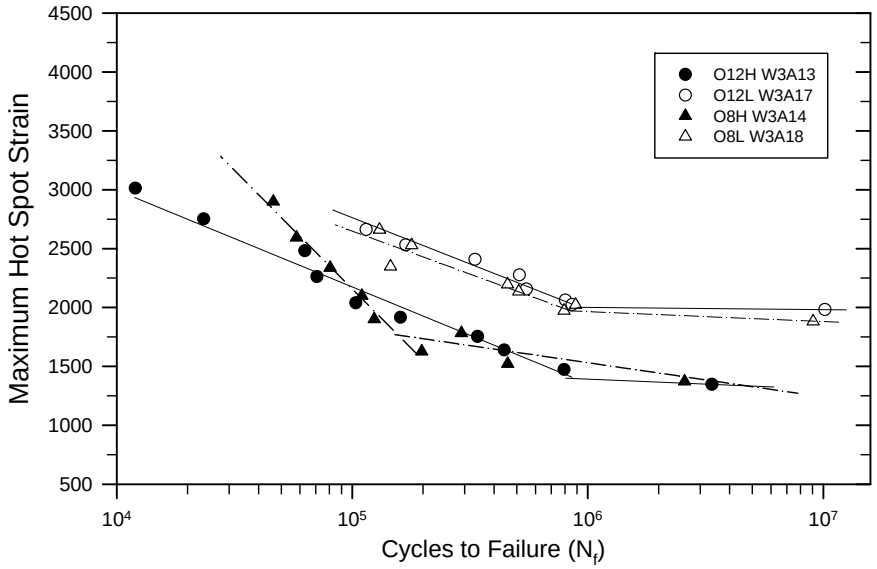

Figure 5: Hot spot strain fatigue life curves for welds made with the overmatched filler metal.

Defects at welds can substantially reduce fatigue life and the intention in this work was to assess whether intrinsic relationships can be found between fatigue performance and the hardness and residual strain gradients acting at the weld toe. It was therefore necessary to inspect the fracture surfaces to determine whether crack initiation had been unduly influenced by weld defects. In such cases the result from that specimen would be excluded when fitting regression lines to the fatigue data. In the event, the only defect observed was undercut at the weld toe in a very small number of specimens and these data were excluded from the regression process.

The hot spot strain fatigue ranking order at lives of 10^5 and $2x10^6$ cycles is shown in Figure 6. With reliable data established for fatigue ranking using hot spot strain, for residual strain and for microhardness it is possible to explore physically meaningful ways of relating the strain and hardness gradients across the weld toe region to the fatigue performance of the various welds. From such data it should be possible to identify weld conditions and parameters that permit fabrication of higher performance welds. The section below outlines the approach taken in this work towards this goal and more complete details are contained in [14].

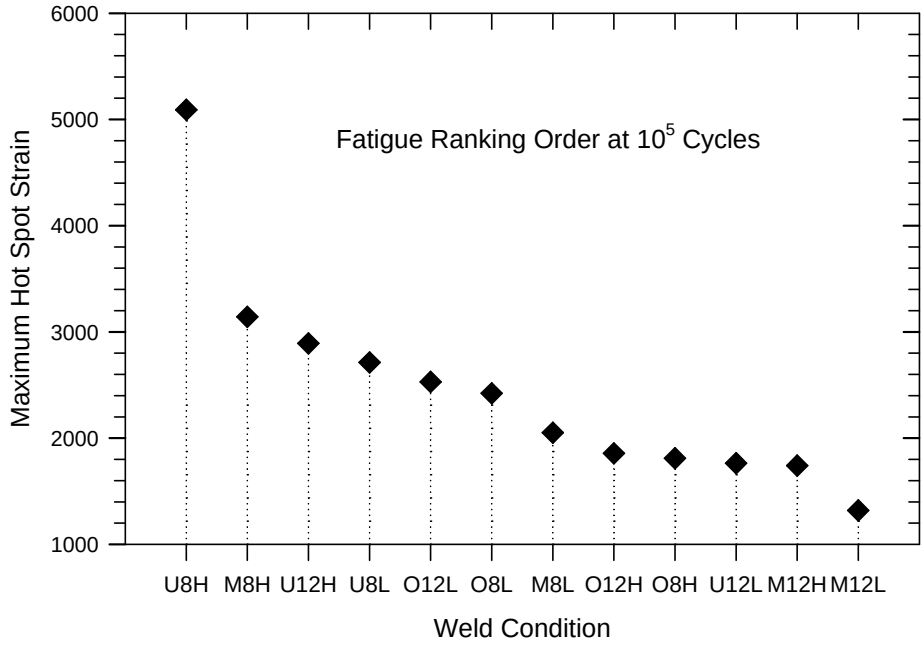

Figure 6a: Fatigue ranking order for the welds at a life of 10^5 cycles as a function of hot spot strain.

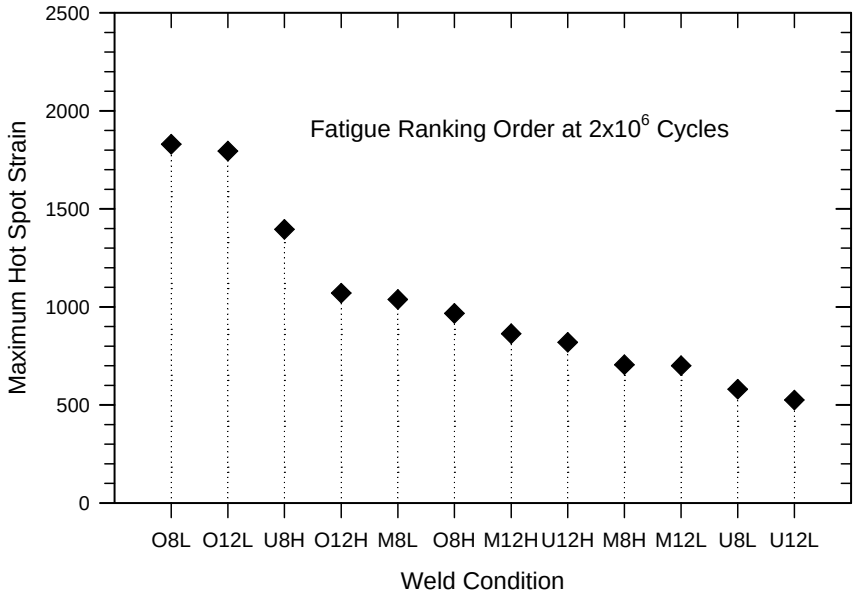

Figure 6b: Fatigue ranking order for the welds at a life of $2x10^6$ cycles as a function of hot spot strain.

7. PREDICTING FATIGUE RANKING

If the fatigue performance correlates directly with transverse residual strain across the weld zone, there are a number of possibilities for parameters that might be relevant, particularly as

the weld toe is often close to a turning point in the residual strain profile. These include the gradients of the profile segments either side of the turning point, the magnitudes of the strain change associated with these segments, the change of gradient across the weld toe and the angle between the two segments. These parameters are also different at the two weld toes and hence the "worst" case (or most severe parameter) was used in the modelling. The same comments apply to the microhardness profiles. All of these cases were considered in the modelling process. The difficulty of reaching generalised conclusions regarding residual strain and microhardness gradients resulting from the use of particular filler metals, heat input of plate thickness, is discussed in reference 14 which presents data for the maximum weld toe hardness gradient for the weld conditions tested in this work. No clear trends are apparent from such data considered independently from other parameters, although some generalised some observations can be made. The variability in such data emphasises the problems faced in research work aimed at developing improved understanding of relationships between weld process parameters, microstructural and strain properties and fatigue performance.

Once all the gradient and magnitude data required for modelling had been extracted from the residual strain and hardness profiles it was plotted against the fatigue ranking order given in Figure 6 for the two fatigue lives of interest. The interest here was to determine whether any clear trends in data could be observed that would allow prediction of fatigue ranking directly from conjoint consideration of strain and hardness profiles across the weld toe. If such relationships could be established there is then the possibility of significant simplification in future work aimed at interpreting *process-property-performance* relationships for welds in higher strength steels.

The initial concept used in the modelling explored the possibility of taking middle-ranking weld conditions as representing some "average" of particular gradient and magnitude parameters and seeking to identify a method of predicting the deviation of particular welds from this average that correlated with the observed fatigue ranking order. This approach did not yield any useful outcomes and the possibility was therefore explored of identifying fatigue performance from trends in the strain and hardness data (gradient, magnitude and range). It might then be possible to assess the relative fatigue performance of various weld conditions from simple line profile measurement of residual strain and microhardness.

Figure 7 shows the prediction of hot spot strain obtained with the most successful discrimination procedure found in this work, which is fully discussed in [14]. It allows prediction of hot spot strain for 10/12 of the weld conditions at a fatigue life of 10^5 cycles. It combines the maximum weld toe range of hardness at mid-depth in the specimens with the maximum range of weld toe residual strain at a depth of 1 mm. The excluded weld conditions are at the two extremes of the fatigue ranking, i.e. U8H and M12L. Equation 1, repeated from reference 14, gives the three relationships found between hot spot strain and range of hardness at mid-depth, using residual strain range at 1 mm depth as the discriminator.

An underlying physical rationale for these relationships could invoke the influence of the near-toe residual strain on mean stress and hence plastic deformation in the toe region, and the control of crack growth (in this relatively low life regime) by bulk hardness properties rather than near-surface properties.

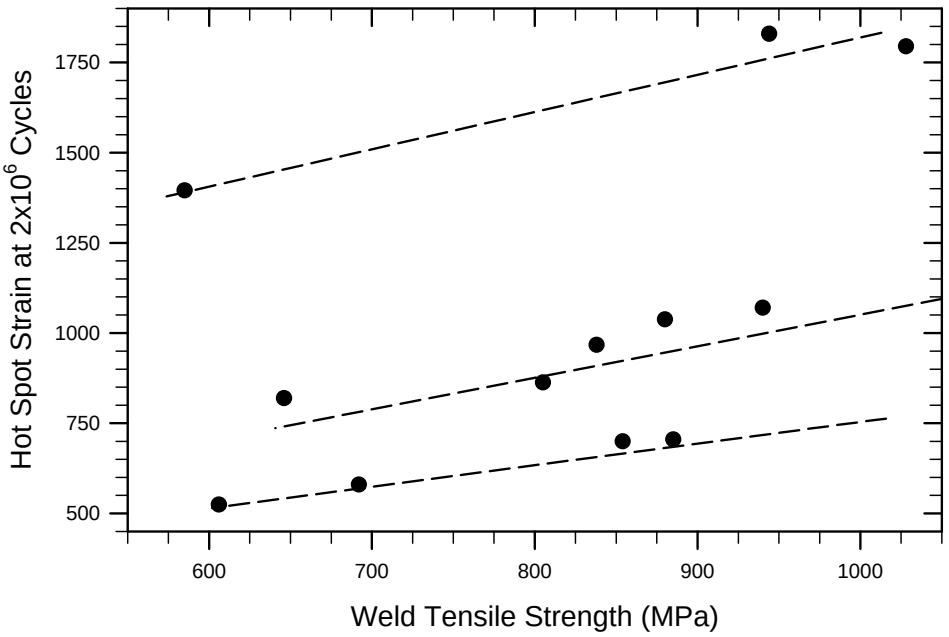

Figure 7: Prediction of hot spot strain for the welds at a fatigue life of 10^5 cycles achieved using a combination of range of residual strain at 1 mm and range of hardness at mid-depth.

$$\begin{aligned} Hot\ Spot\ Strain &= 15.2\,\Delta HV + 1579 \quad if\ \Delta\mu\varepsilon \leq 1425 \\ Hot\ Spot\ Strain &= 11.2\,\Delta HV + 1661 \quad if\ 1425 < \Delta\mu\varepsilon \leq 1650 \\ Hot\ Spot\ Strain &= 2.6\,\Delta HV + 1607 \quad if\ \Delta\mu\varepsilon > 1650 \end{aligned} \tag{1}$$

Prediction of the fatigue performance of the welds at a life of $2x10^6$ cycles was less successful as, although linear correlations could be achieved for groups of welds by plotting weld tensile strength against hot spot strain (12/12) it was not possible to identify a way of discriminating between the welds in each group using second parameter. This is a surprising result, as crack initiation and early growth will be more important to overall fatigue performance in the high cycle regime and would thus be expected to correlate with residual strain. It is possible, however, that residual stress would provide a good discriminator. Calculation of stresses requires knowledge of strain components in three directions and is the subject of ongoing investigation.

Acknowledgements

Support by Corus through the Swindon Technology Centre, of a CASE award for S-P Ting is gratefully acknowledged. Neutron strain scanning was performed at the ILL, Grenoble through the award of beam time under experiment 7-01-196 with the support of Dr D Hughes; the assistance of Dr L Edwards (Open University) and Dr A Evans (ID31 instrument at the ESRF) with the d_0 measurements on toothcomb specimens of the steel welds is also gratefully acknowledged.

References

[1] British Standard BS 7608 : 1993, Code of Practice for Fatigue Design and Assessment of Steel Structures, British Standards Institution, London, ISBN 0 580 212815, 1993.

[2] Kandil, F.A., Lord, J.D., Fry, A.T. and Grant, P.V. (2001) A review of residual stress measurement methods - a guide to technique selection. National Physical Laboratory Report MATC(A)04, Teddington, UK.

[3] Withers, P.J. and Bhadeshia, H.K.D.H. (2001) Residual stress: Part 1 – measurement techniques. Mater. Sci. Engng **17**, 355-365.

[4] Withers, P.J., Turski, B., Edwards, L., Bouchard, P.J. and Buttle, D.J. (2008) Recent advances in residual stress measurement. Int. J. Pressure Vessels and Piping **85,** 118–127.

[5] Lachmann, C., Nitschke-Pagel, T. and Wohlfahrt, H. (2000) Characterisation of residual stress relaxation in fatigue loaded welded joints by X-ray diffraction and Barkhausen noise method. Proceedings of the 5th European Conference on Residual Stresses, Delft-Noordwijkerhout, The Netherlands, September 29-30, 1999. Edited by A.J. Böttger, R. Delhez and E.J. Mittemeijer, Materials Science Forum (2000) **347-349**, 374-381.

[6] Zhuang, W.Z., Halford, G.R. (2001) Investigation of residual stress relaxation under cyclic load. Int. J. Fatigue **23** S31-S37.

[7] Bouchard, P.J. (2008) Residual stresses in lifetime and structural integrity assessment. Encyclopedia of Materials: Science and Technology, 8134-8142**.**

[8] Lassen, T. and Recho, N. (2009) Proposal for a more accurate physically based S–N curve for welded steel joints. Int. J. Fatigue **31**, 70-78.

[9] Chien-Yuan Hou (2007) Fatigue analysis of welded joints with the aid of real three-dimensional weld toe geometry. Int. J. Fatigue **29**, 772-785.

[10] Toyosada, M., Gotoh, K. and Niwa, T. (2004) Fatigue life assessment for welded structures without initial defects: an algorithm for predicting fatigue crack growth from a sound site. Int. J. Fatigue **26**, 993-1002.

[11] Almer, J.D., Cohen, J.B. and Moran, B. (2000) The effects of residual macrostresses and microstresses on fatigue crack initiation. Mater. Sci. Engng **284**, 268-279.

[12] Guozheng Kang (2008) Ratchetting: Recent progresses in phenomenon observation, constitutive modeling and application. Int. J. Fatigue **30**, 1448–1472.

[13] James, M.N., Webster, P.J., Hughes, D.J., Chen, Z., Ratel, N., Ting, S.-P., Bruno, G. and Steuwer, A. (2006) Correlating weld process conditions, residual strain and stress and mechanical properties for high strength steel – the role of neutron diffraction. Mater. Sci. Engng A, **427,** 16-26.

[14] James, M.N., Ting, S.-P., Bosi, M., Lombard, H. and Hattingh, D.G. (2009) Residual strain and hardness as predictors of the fatigue ranking of steel welds. Submitted to Int. J. Fatigue.

[15] Hughes, D.J., James, M.N., Hattingh, D.G. and Webster, P.J. (2003) The use of combs for evaluation of strain-free references for residual strain measurements by neutron and synchrotron X-ray diffraction. J. Neutron Res. **11**, 289-293.